

## Article

# Classification of Different Brain Dynamics Associated to Different Cognitive Modalities: Towards an Understanding of Self-willed Generated Cognitive States

Jeffery Jonathan Joshua (ישיוע) Davis<sup>\*1</sup> & Sungchul Ji<sup>2</sup>

<sup>1</sup>The Embassy of Peace, Whitianga, New Zealand

<sup>2</sup> Ernest Mario School of Pharmacy, Rutgers University, Piscataway, NJ, USA

## Abstract

In recent years the Planckian distribution was introduced by [1] to characterize biophysical oscillatory processes that generate distributions similar to the Planck radiation equation, Planck's law [2, 3]. In the Planck radiation equation, temperature (T) plays a fundamental role in shaping the spectrum distribution. Here we apply the Planckian distribution equation to model different brain states presumably associated to different cognitive states, where we propose that the generalized parameters of the Planckian distribution equation could act as predictors of the distribution shape and the brain states analogous to the role of temperature (T) in the Planck equation. In our case we propose that the parameters could be associated to the power of will, attentional focus or commitment to a way of being with certain associated brain dynamics and we show the different distributions associated to brain data collected for twenty (20) participants, in meditation/relaxation or an engaged audio-visual task. We conclude that even though brain dynamics as described by *Ji's Planckian distribution (JPD)* in fMRI studies have been successful when measuring EEG signals in humans, the JPD shows to be limited in characterizing the experimental power spectrum recorded for multiple participants in the two (2) modalities analyzed. However, the Gaussian and Lorentzian distributions do fit the data and significantly succeed in characterizing the data, even in the case of bi- or multi-modality, when combining two (2) or more Gaussian or Lorentzian distributions.

**Keywords:** Planckian distribution, Planck's law, EEG, brain dynamics, mind, intentional action.

## 1. Introduction

One of the most difficult challenges for science, and particularly for cognitive science, has been to elucidate whether the brain creates the mind or mind belongs to a different domain, a fundamental domain that is either in a form of symbiosis or in a kind of unity with the functioning of the human brain, something very little understood till now. Far from attempting a philosophical resolution to this dilemma that includes, amongst others: (a) the dual-aspect theory of Aristotle [4], (b) Aquinas' endorsement of Aristotle [5], however, with his own distinctions between soul, mind, body and intentionality, (c) Cartesian Dualism [6], (d) Kant's Dualism and transcendental idealism [7, 8], (e) the neutral monism of Baruch Spinoza [9] and more recently

\*Correspondence: c/o Sarah Frew, The Embassy of Peace, Whitianga, New Zealand. E-mail: science@theembassyofpeace.com

Note: This article was first published in *Journal of Consciousness Exploration & Research* 14(5): pp. 424-442 in October, 2023.

(f) Merleau-Ponty's intentionality of consciousness that incorporates the natural and the transcendental, together with his treatment of Gestalt as "a spontaneous organization of the sensory field" [10], we prefer to address this dilemma based on experimental data and the physics of oscillatory systems, as well as veridical reports from people about their intentions, commitments, meanings and values, reflected in brain dynamics, verbal utterances, written reports, written contracts and behavior.

When trying to deeply and scientifically understand the mind~brain complementarity as Kelso puts it with the aid of the symbol ( $\sim$ ) [11], we have drawn inspiration from the work of giants like:

- (a) Karl Pribram, who supported an ontological monism vis-à-vis an epistemological dualism, where "*Brain is material, communication is mental*", employing concepts like Sensory Generated Receptive Fields and Quanta of Information [12-17].
- (b) John Eccles, who supported an ontological dualism, where concepts like dendrons in the brain and psychons in the mind, play a role in mind~brain dynamics [18].
- (c) Walter Freeman, who derives from Aquinas [19] and Merleau-Ponty [20] his foundational approach to the mind-body relationship via a comprehensive systems neuroscience that integrates classical fields, semiosis, intentionality and pragmatic information, in order to explain body (brain)~environment transactions via the action perception cycle and Merleau-Ponty's intentional arc [21-30].

All these years of explorations have led us, together with others, to the publication of several research studies where we applied quantitative methodologies to understand brain dynamics, both in animals and humans [31-34], and more recently, to explore the different psychophysiological states that a human being can generate at will, affecting his or her brain and heart dynamics [35, 36]. Usually, our methodologies involved the computation of the power spectrum and the Hilbert transform in different bands [37]. However, only days before the decision of producing this study-report I, Joshua, one of the authors, had an insight into how relevant Ji's Planckian distribution (JPD), as I have proposed to call the Planckian distribution proposed by Ji [1], could be in describing different brain dynamics, presumably associated to different mental states, intentions, meanings and plans of action, and the role that Ji's equation can play when investigating the mind as the subjective part and the brain as the objective counterpart of an intentional complementary mind~brain system that supports human values based decision making.

Ji's Planckian distribution may be limited to fit some power spectrum-based distributions only, obtained from brain dynamics in EEG human recordings. However, because of its success when analyzing brain data in fMRI studies as noted by Ji, the JPD model could serve as an initial model to build on. The fMRI data sets were measured by Carhart-Harris when studying the effect of psilocybin in cerebral blood flow, as shown in [38] (p. 366).

Here we briefly revisit Planck's law and will also explain the generalized version proposed by Ji, Ji's Planckian distribution, and will apply the JPD to the analysis of brain data collected from twenty (20) participants, via EEG, contrasting two (2) experimental modalities: meditation and watching a music video with ambiguous images.

We show our results contrasting the power of classification of the JPD with the Gaussian and Lorentzian distributions, as well as their application to model and explain an intentional complementary mind~brain system that supports human values and meanings geared towards survival, cultural, aesthetic and spiritual values based decision making.

## 2. An Introduction to Planck’s Law

Before we introduce the reader to Ji’s equation, it is imperative to revisit the Planck radiation equation that has been fundamental in explaining black body radiation [2, 3].

It was Max Planck in his ‘Eight Lectures on Theoretical Physics’ delivered at Columbia University in 1909, as well as in a revised translation by Planck and Masius of Planck’s book titled, ‘The Theory of Heat Radiation’ (1914), that this equation was introduced to the physics community in order to deal with the Ultraviolet Catastrophe (Rayleigh–Jeans catastrophe), as a consequence of the limited model for radiation provided by Rayleigh–Jeans law. Rayleigh–Jeans law failed to provide accurate predictions for radiation approaching the ultraviolet region of the electromagnetic spectrum.

The Planck radiation equation is as follows:

$$B(\lambda, T) = (2\pi hc^2 / \lambda^5) / (e^{hc/\lambda kT} - 1) \tag{1}$$

where  $\lambda$  is the wavelength and T is the temperature, and where  $\pi$ , h, k and c are all well-known constants in the field of physics. Basically, this general equation produces different spectrums for different temperatures (T), as shown in Figure 1.

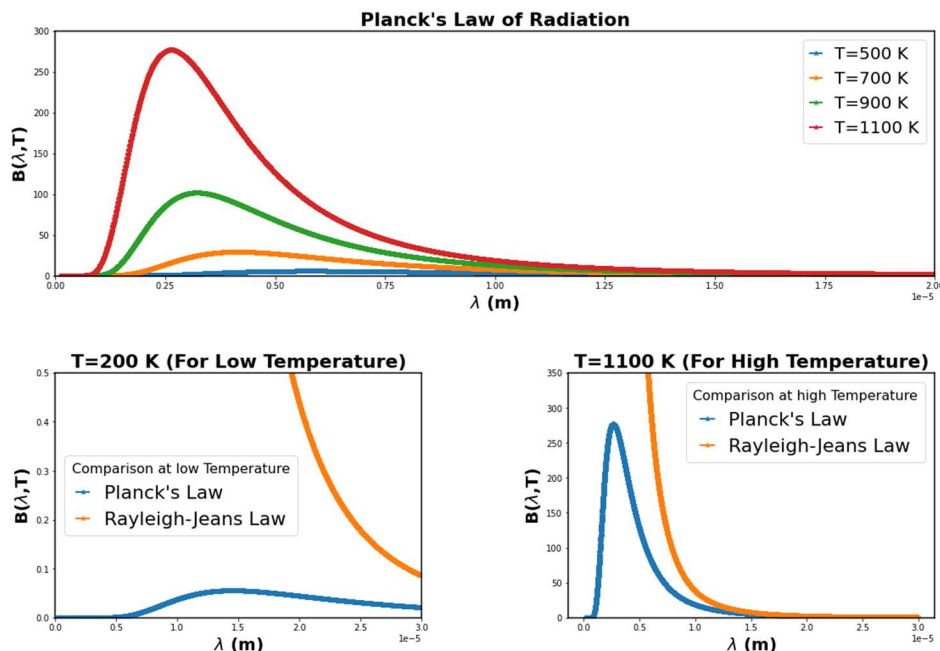


**Figure 1.** Planck’s law for four (4) different temperatures (top), Comparison between Planck’s law and Rayleigh-Jeans law for relatively low temperatures (bottom left) and relatively high temperatures (bottom right).

### 3. Introduction to Ji’s Planckian Distribution

Now that we have introduced Planck’s law, we can explore a general form of this equation introduced by Ji in [1], in order to model different biophysical phenomena, processes or systems [38]. If we make  $\lambda = (x+B)$ ,  $A = 2\pi hc^2$  and  $C = hc/kT$ , we can transform Planck’s radiation equation into the following isomorphic equation:

$$S(x, C) = \frac{A}{(x+B)^5} * \frac{1}{e^{C/(x+B)} - 1} \tag{2}$$

where A and B are constants and C can be regarded as a control variable replacing T in oscillatory biosystems different from the one generating the black body radiation. This equation we will refer to as Ji’s Planckian distribution (JPD) from now on.

The brain generates oscillations at different frequencies, usually studied between 2-48 Hz, via the power spectrum or the Hilbert transform in different bands [30, 34, 37]. This means that the power spectrum of brain signals measured on the scalp or the cortex of a human being, for example, could in principle be modeled by the JPD. In Figure 2 below, we show the power spectrum of a human being measured in two (2) different activities via EEG recordings: meditation and watching a music video with ambiguous images.

We can observe the difference between the power spectrum obtained from measurements in both activities, where the power spectrum in a meditation shows significantly more power than in the activity of watching a video in the Alpha band (~10 Hz). Another characteristic of both power spectrums is the bi-modality, where a small peak power can be visually observed in the Beta band (~18 Hz). If this bi-modality can be eliminated or addressed by treating the power spectrum of each brain area independently, for example, or by combining the dynamics of different brain areas with a sum of JPDs, then one can characterize brain dynamics, in different relevant areas, associated with the different cognitive states (a) and (b), as shown in Figure 2, by varying the free parameters A, B and C.

Power Spectrum derived from human EEG measurements in:

(a) meditation and (b) watching a music video

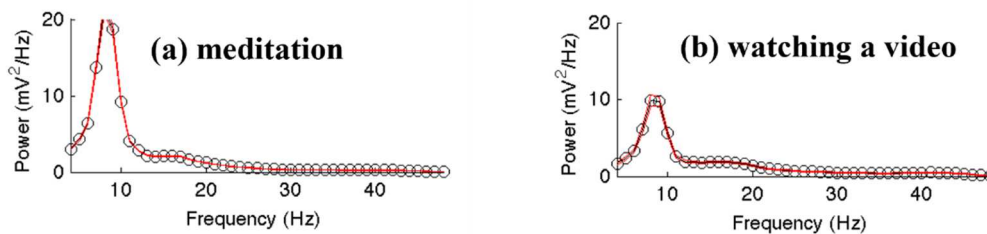


**Figure 2.** It shows the power spectrum derived from EEG recordings for one participant in the modalities of (a) meditation and (b) watching a music video with ambiguous images.

Note that in this biosystem, frequency (Hz) replaces wavelength ( $\lambda$ ) and C replaces  $hc/kT$  or  $\mu/T$ , where  $\mu$  is a constant and T is a parameter variable (variable is x, not T) different than Temperature. It follows that we can rewrite the JPD as:

$$S(x, T) = \frac{A}{(x+B)^5} * \frac{1}{e^{\mu/T/(x+B)} - 1} \quad (3)$$

The most interesting part for us is that a general parameter T (different from temperature) in the case of the mind~brain system, could be related to a subjective mental decision variable associated with will, intention and commitment, as in, for example, the decision to meditate or to enjoy a music video, and to plan for both activities. This subjective value and meaning based decision variable, in principle, could produce two (2) different kinds of brain dynamics distributions, one (1) for each modality, that could be modeled with the JPD by varying T, in other words, by changing one's mind, intentions, attention and focus. This is analogous to the modeling of black body radiation when we vary Temperature (T) in Planck's radiation equation, however, T in the case of the sun for example, is fixed and the sun has no means to consciously change its temperature at will, since it is just a natural fusion reactor with no conscious will or conscious operators to change its T parameter. Perhaps, to avoid confusion with the use of T for temperature in Planck's radiation equation, we could label our subjective and mental decision variable as M, and the equation would be rewritten as:

$$S(x, M) = \frac{A}{(x+B)^5} * \frac{1}{e^{\mu/M/(x+B)} - 1} \quad (4)$$

In doing so we have produced an equation to model, in a complementary fashion, the subjective~objective aspects of the mind~brain system, and we can test this model empirically by allowing such a subjective choice to be defined as an act of will or a commitment to intentionally act towards meditation or watching a video, for example, according to each experimental condition and paradigm to be tested. This, of course, should never be limited to the JPD, since any other model with similar features could do the job, and a set of models and equations could give us flexibility in modeling different biological systems like the brain, when measured via different instruments and observables, such as EEG and fMRI to name a few, in order to properly characterize different cognitive states with their subjective, intentional and mental soft variables.

Furthermore, by hypothesizing M to be the cause of a form of energy (E) to express in brain dynamics, as for example, M causing the excitation or inhibition of neurons, we could also derive such an energy variable E(M) to be a function of our subjective and mental decision variable M, leading to an equation that could model the mental~neuro-energetics of different intentionally driven cognitive states. Such an equation could be written as:

$$S(x, E(M)) = \frac{A}{(x+B)^5} * \frac{1}{e^{\mu/E(M)/(x+B)} - 1} \quad (5)$$

This study will be limited to the application of equation (4), to analyze brain data from the perspective of a complementary mind~brain system. The model of equation (5) to describe the mental~neuro-energetics of different intentionally driven cognitive states will be left for future studies.

## 4. Experimental Setting

This study was conducted in Ian J. Kirk's Lab, Centre for Brain Research at The University of Auckland in New Zealand, during a period of about three (3) months of data acquisition. This work focuses on two (2) modalities: (a) Meditation-Relaxation (MED) and (b) Video Watching (VDO). We measured twenty (20) participants, of which eleven (11) were Meditators and nine (9) Non-Meditators.

We used a HydroCel Geodesic Sensor Net (HCGSN) with 128 electrodes, which is a dense-array electroencephalography (EEG) technology produced by Electrical Geodesics, Inc. To program the experimental sequence and general settings we used E-Prime 2.0 that allowed for the tracking of the different events of interest from the presentation of stimuli, as well as other relevant events, like 'start' and 'press key'.

The participants sat inside a Faraday chamber in front of a computer screen with a keyboard. They used only the space bar and the numerical keypad and were shown how to restrict head and eye movement to minimize artifacts while data recording. We conducted three (3) impedance checks: (a) before the experiment began, (b) after the first block of experiments comprised of two (2) modalities, and (c) after the second block of experiments comprised of two (2) other modalities. The experiment concluded with the third block of experiments where we measured the last two (2) modalities.

For the modality of meditation (MED), conducted in the first experimental block, participants were given the task to meditate using any practice of their choice for seven (7) minutes, with their eyes closed. If the participant was unfamiliar with meditation, they were given the task to relax with their eyes closed.

For the modality of video watching (VDO), the final modality in the third experimental block, the participants were asked to watch and listen to a video with ambiguous images and the song 'Imagine' by John Lennon. Both modalities were considered passive in the sense that neither of them required an evaluative action or response via the keyboard.

The participants were all healthy, eleven (11) males and nine (9) females, within an age range of twenty-three (23) to sixty-four (64) years. Participants were grouped as meditators, when they have been meditating regularly for at least five (5) days a week, for at least two (2) years. The rest of the participants were grouped as non-meditators.

## 5. Signal Processing, Analytic Methods and Computations

The data was recorded using a Net Station 4.4.2 (Electrical Geodesics Inc. Eugene, Oregon, USA) at a sample rate of 1000Hz. The signals obtained from the 128 electrodes were computationally treated as a 1D-vector with 128 elements and after pre-processing were reshaped into a 12 x 12 matrix (A) with 144 elements, configured according to different brain areas. Some electrodes were doubled to fill the matrix. The matrix elements A(1, 3) and A(1, 10) were left empty as reference points for the position of the pre-frontal cortex, as shown in Figure 3.

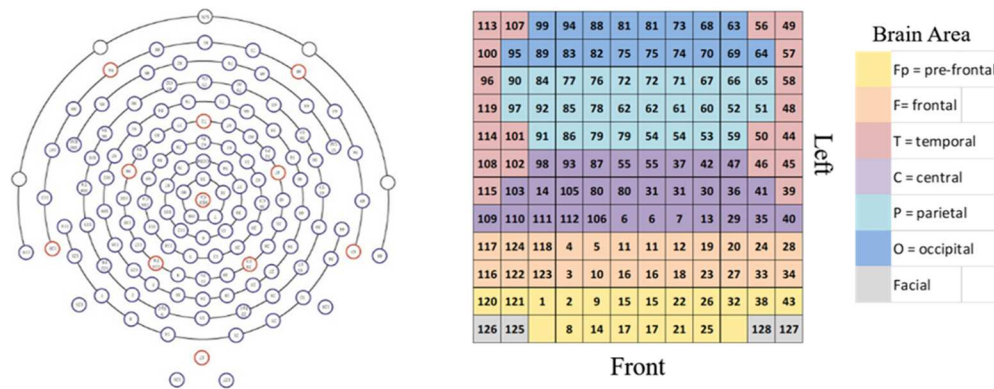


**Figure 3.** Illustration of electrode arrangements; (left) displays the EEG electrode positions and numbers, and (right) shows a representation matrix (A) of 12x12 for the 128 EEG electrodes in the sensor net over the whole scalp, with a few electrode positions being repeated to fill the matrix array. Brain areas are described according to color and electrodes, as shown in the legend. The left and right hemispheres are represented by two (2) equal and symmetrical parts of size 12x6 each. Positions A(1, 3) and A(1, 10), starting from the bottom left, are empty.

In order to remove artifacts derived from blinking and other body movements, the EEG signals were further pre-processed as described in [34], where a notch filter for 50 Hz removal was used, hand in hand with finely tuned filter and detrend algorithms that resulted in a reliable data set with a spectrum between 2-48 Hz.

Finally, we computed the temporal power spectrum (PSDt) over time windows of 500 ms, where t varies from 1 to number of windows (N), for each electrode. Such power spectrum was transformed into a normalized probability function (histogram) that was fitted to the Gaussian, Lorentzian and JPD equations via an optimization algorithm with the aid of Python. This was done for a pair of distributions in order to capture the characteristics of the power spectrums when showing bi-modality, something that the Gaussian equations captured better than the Lorentzian and JPD equations for many participants, as shown in Figure 4. This allowed us to compute parameters of the JPD for any desired PSDt, as well as conducting further statistical analysis to classify the different behaviors of the two (2) modalities studied, and finally draw some relevant conclusions.

The models that we fit to the experimental power spectrum are: (a) Ji’s Planckian Distribution - JPD(x), (b) Gaussian Function - G(x), and (c) Lorentzian Function - L(x).

The equations are as follows:

$$JPD(x) = \frac{A1}{(x+B1)^5} * \frac{1}{e^{C1/(x+B1)} - 1} + \frac{A2}{(x+B2)^5} * \frac{1}{e^{C2/(x+B2)} - 1} \tag{6}$$

$$G(x) = A1 * e^{-\frac{(x-\mu1)^2}{2*\sigma1^2}} + A2 * e^{-\frac{(x-\mu2)^2}{2*\sigma2^2}} \tag{7}$$

$$L(x) = A1 * \frac{0.5*w}{(x-\mu)+(0.5*w)^2} + B1 + A2 * \frac{0.5*w}{(x-\mu)+(0.5*w)^2} + B2 \tag{8}$$

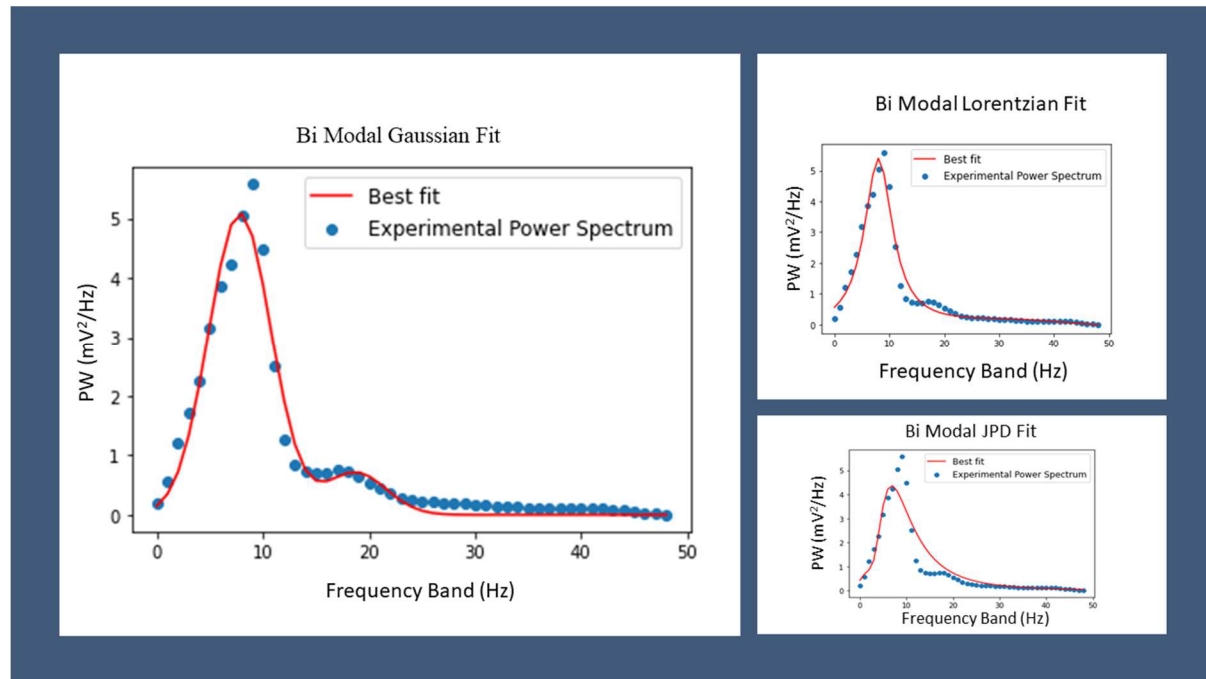


**Figure 4.** It shows Bi-Modal Fits of the Gaussian, Lorentzian and JPD distributions for the Experimental Power Spectrum for one participant in the MED modality, where the Gaussian equations capture the features of the Power Spectrum the best.

Qualitatively we can observe in Figure 4 that the Lorentzian and the Gaussian Fits seem more representative of the Experimental Power Spectrum than the JPD.

Then we estimate the mean  $\mu_H$  and  $\sigma_H$  standard deviation from the **Shannon Entropy indices** ( $H_i$  with  $i=1,20$ ), as well as the mean  $\mu_{PSk}$  and  $\sigma_{PSk}$  standard deviation for the **Pearson’s First Skewness Coefficient** ( $PSk_i$ ) of each of the twenty (20) participants, based on the Normalized Experimental Power Spectrum and the optimal fits for  $L(x)$ ,  $G(x)$  and  $JPD(x)$ , all turned into probability distributions, as shown in Figure 5.

The poor fitting of JPD evident in Figure 5 could be addressed by considering that:

- (i) The Alpha band (8-12 Hz) is negatively skewed, which has been found to fit to JPD with a greater difficulty than positively skewed distribution. In other studies, negatively skewed histograms were found to fit better the 4-parameter version of the JPD  $S(x, b) = \frac{a/(A+Bx)^5}{e^{b/(A+Bx)} - 1}$ , as shown in Figure 6.
- (ii) The Beta band (13-25 Hz) is positively skewed so that, when it can be isolated from the predominant Alpha band, it may fit to JPD much better than shown.

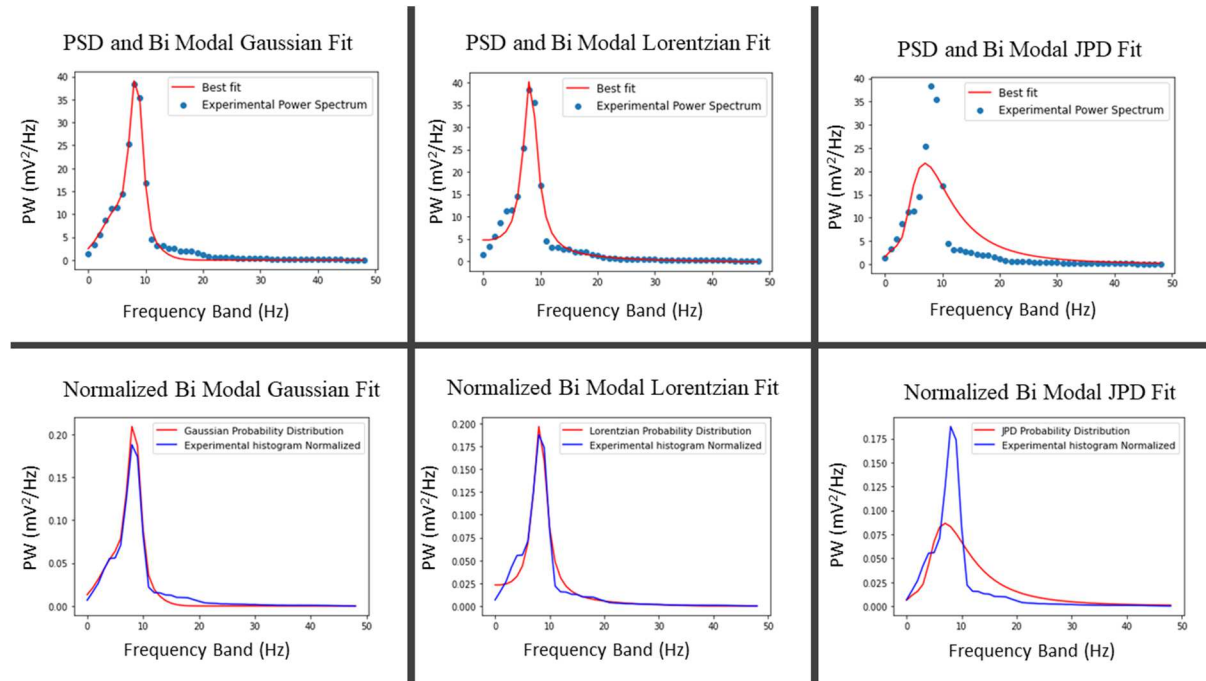


**Figure 5.** It shows (a) comparative set of Gaussian, Lorentzian and JPD optimal fits for the Experimental Power Spectrums (top row), and (b) Normalized Power Spectrum for Experimental and Optimal Fits for Gaussian, Lorentzian and JPD (bottom row). This data comes from Participant 20 in the MED modality.

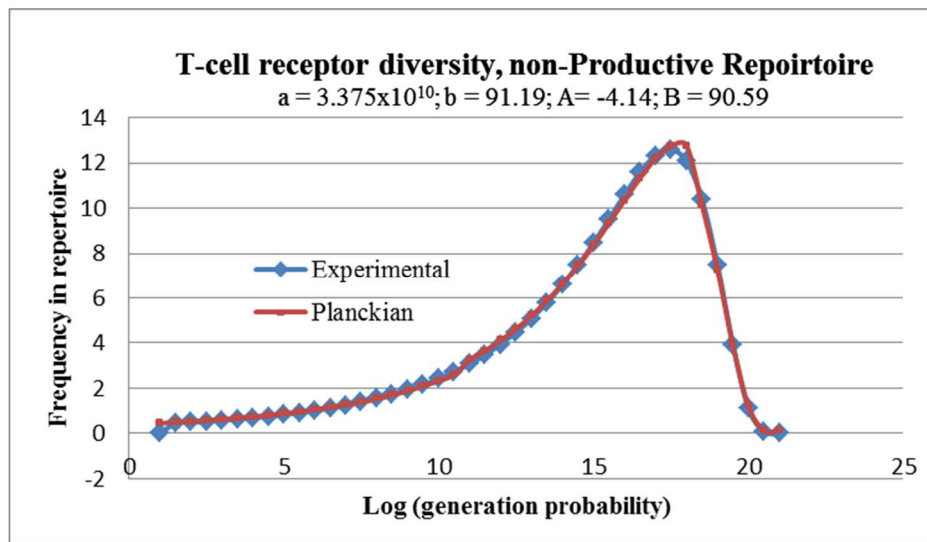


**Figure 6.** It shows an example of the four (4) parameter versions of the JPD reproduced from [38] (pp. 343, 350-351)

From the power spectrums we derive the Shannon Entropy Index (H) and the Pearson’s First Skewness Coefficient (PSk) that we use to compare the modalities of MED and VDO.

Following we present the equations to compute the Shannon Entropy index (H), as follows:

$$H = -\sum_{i=1}^n p_i * \log_2(p_i) , \text{ where } p_i = \frac{PW_i}{TP} \quad (9)$$

$PW_i$  corresponds to the power of frequency band ‘i’, TP is the total power, computed as:

$$TP = \sum_{i=1}^n PW_i \tag{10}$$

The equation for the computation of PSk is:

$$PSk = \left| \frac{(Mean_{PSD_t} - Mode_{PSD_t})}{SD_{PSD_t}} \right| \tag{11}$$

where  $PSD_t$  as mentioned above, is computed as:

$$PSD_t \doteq PW_i (FB_i), \forall i \tag{12}$$

where i stands for the  $i^{th}$  band and in every window t, usually of 500 ms,

and where  $SD_{PSD_t}$  represents the standard deviation of the  $PSD_t$ , and, where power is taken as a function of frequency and therefore frequency band, described here as  $PW_i(FB_i)$ .

## 6. Results & Analysis

In this section we show the results of our experiments, aiming at:

- (a) characterizing the Experimental Power Spectrum in the modalities of MED and VDO with three (3) potential candidate equations  $G(x)$ ,  $L(x)$  and  $JPD(x)$ .
- (b) comparing the two (2) modalities via H and PSk to capture any difference in brain dynamics and brain states between modalities.

In order to perform relevant statistical tests, we define  $H_{t,e}^{p,m}$  as a value of H derived from the PSD in window t, for participant p, in modality m, for electrode e, where NW, the number of windows in which we compute  $PSD_t$ , is computed as  $NW = \frac{L}{500}$ , with L being the time length (in ms) of a particular experiment for participant p in modality m, and where, as stated before, the length for each window t equals 500 ms.

The mean value of H over all windows, per electrode, per participant, per modality, is computed as follows:

$$\bar{H}_e^{p,m} = \sum_{t=1}^{NW} \frac{H_{t,e}^{p,m}}{NW} \tag{13}$$

Then we compute the mean value  $\bar{H}_e^{p,m}$  over all electrodes, per participant, per modality, as follows:

$$\bar{\bar{H}}^{p,m} = \sum_{e=1}^{128} \frac{\bar{H}_e^{p,m}}{128} \tag{14}$$

Finally, we define the mean value of H per group, per modality, as follows:

$$\bar{H}_g^m = \sum_{p=1}^{npg} \frac{\bar{\bar{H}}^{p,m}}{npg} \quad \forall g = 1, 2 \tag{15}$$

In the above formula, the degrees of freedom (df) are defined as  $npg$ , which equals the number of participants per group, eleven (11) for the Meditator group ( $g=1$ ), nine (9) for the Non-Meditator group ( $g=2$ ), and for All the twenty (20) participants ( $g=3$ ). Similarly, we computed the standard deviation for the value of H per group, per modality and have labeled it as  $Hs_g^m$ , from which we can derive the interval of confidence for  $\bar{H}_g^m$ , as follows:

$$\bar{H}_g^m \pm t_{\alpha=0.05, npg} * \frac{Hs_g^m}{\sqrt{np g}} \quad (16)$$

It is important to note that the above formulas similarly apply to the computation of  $\overline{PSk}_e^{p,m}$ ,  $\overline{PSk}^{p,m}$ ,  $\overline{PSk}_g^m$  and  $PSks_g^m$ . These formulas can be easily adapted to different brain areas by including only the corresponding electrodes.

In Table I we show the H mean values and confidence intervals with  $\alpha = 0.05$  for the modalities of MED and VDO, for all twenty (20) participants, for the experimental data and the Gaussian, Lorentzian and JPD optimal fits. It seems clear that the mean value of H associated with the JPD fit for the MED modality, is significantly greater than the mean values of H computed for the experimental data, and the Gaussian and the Lorentzian optimal fits when normalized as probability distributions. This is indicative of a poor JPD fit for the experimental power spectrums of most participants when visual inspection was applied, as shown in Figures 4 and 5, and in general, as shown in the statistical analysis in the following tables.

**Table I.** It shows the intervals of Confidence for the mean values of H based on the Experimental, Gaussian, Lorentzian and JPD distributions derived from the respective Power Spectrums.

	<b>MED</b>	<b>VDO</b>
<b>H from Experimental data</b>	4.3626 ± 0.2293	4.8984 ± 0.1615
<b>H from Gaussian fit</b>	4.1254 ± 0.2924	4.8408 ± 0.2062
<b>H from Lorentzian fit</b>	4.4029 ± 0.2331	4.9368 ± 0.3486
<b>H from JPD fit</b>	4.6797 ± 0.1311	4.8370 ± 0.1171

Two important observations are derived from this analysis:

- we can distinguish between the modalities MED and VDO very well when comparing the values of H based on the experimental data, the Gaussian, the Lorentzian and the JPD fits.
- we observe, statistically speaking, very similar values for the mean values of H for all the experimental data, and the Gaussian, Lorentzian and JPD, in both modalities showing a tendency for the three (3) models to characterize the experimental data relatively well. However, we can also see that the Gaussian and the Lorentzian equations are better fits than the JPD for the MED modality.
- Similar results apply to the mean values of PSk, as shown in Table II.

**Table II** shows the intervals of Confidence for the mean values of PSk based on the Experimental, Gaussian, Lorentzian and JPD distributions derived from the respective Power Spectrums with their respective parameters, such as the mean, mode and standard deviation for each probability distribution.

	<b>MED</b>	<b>VDO</b>
<b>PSk from Experimental data</b>	0.3582 ± 0.1058	0.6899 ± 0.1177
<b>PSk from Gaussian fit</b>	0.3485 ± 0.1085	0.6645 ± 0.2208
<b>PSk from Lorentzian fit</b>	0.3440 ± 0.0968	0.6550 ± 0.2520
<b>PSk from JPD fit</b>	0.5922 ± 0.0488	0.7046 ± 0.0945

At this stage of analysis, it seems to us that it is relevant and appropriate to back up these observations with more robust hypotheses tests.

We perform tests for two (2) population means to calculate the test statistics, t critical value and the p value, for a given sample size, level of significance with an associated value of  $\alpha = 0.05$ , and for a two-tailed alternative hypothesis.

The relevant formula for the critical value is:

$$t = \frac{(\bar{x}_1 - \bar{x}_2) - (\mu_1 - \mu_2)}{\sqrt{\frac{s_1^2}{n_1} + \frac{s_2^2}{n_2}}} \tag{17}$$

and for the degrees of freedom (*df*) is:

$$df = \frac{(\frac{s_1^2}{n_1} + \frac{s_2^2}{n_2})^2}{\frac{s_1^4}{n_1^2(n_1-1)} + \frac{s_2^4}{n_2^2(n_2-1)}} \tag{18}$$

where,  $\mu_1, \mu_2$  are the population means,  $\bar{x}_1, \bar{x}_2$  are the sample means,  $s_1, s_2$  the sample standard deviations, and  $n_1, n_2$  the sample sizes of modalities 1 and 2 (MED and VDO, respectively) for the H and PSk indexes accordingly.

In Table III below, we present the results of the hypotheses testing for equal means for a set of experiments, where the H mean experimental values for the twenty (20) participants are contrasted with H mean experimental values obtained for the optimal fits of Gaussian, Lorentzian and JPD equations for each participant. This allows a comparison of the modalities of MED versus VDO, as well as the H index, derived from the equations fitted to the experimental power spectrums.

We observe that when using the value of H derived from experimental data, the modalities MED and VDO behave significantly different, showing a p value of 0.000339, much smaller than 0.05, therefore rejecting  $H_0$ .

Similarly, we compare the mean values of H derived from the Gaussian and the Lorentzian models, with the experimentally derived mean H value and we accept  $H_0$ , since there is no

reason to reject the hypothesis for equal H means between the experimental and the fitted models.

For JPD the situation is different, leading us in the direction to conclude that the JPD model poorly characterizes the behavior of H derived from the experimental power spectrum, since we reject H0 when testing for equal means for the values of H derived from the experimental vs. the JPD distributions. Also, when comparing the modalities MED and VDO, we have no reason to reject H0, suggesting that the brain dynamics or states as observed in the modalities MED and VDO and contrasted via the H index, are the same. This is clearly different than for both the Gaussian and the Lorentzian fits, as well as for the experimental probability distribution derived from the power spectrum.

**Table III** It shows the results for the hypotheses tests for equal H means and different variance, for 20 participants with  $\alpha=0.05$ .

TEST	p-value	H0: $\mu_1=\mu_2$
MED vs. VDO (Experimental)	0.000339	Reject
Experimental vs. Gaussian (MED)	0.191372	Accept
Experimental vs. Gaussian (VDO)	0.649211	Accept
MED vs. VDO (Gaussian)	0.000198	Reject
Experimental vs. Lorentzian (MED)	0.798502	Accept
Experimental vs. Lorentzian (VDO)	0.728650	Accept
MED vs. VDO (Lorentzian)	0.000408	Reject
Experimental vs. JPD (MED)	0.017946	Reject
Experimental vs. JPD (VDO)	0.571104	Accept
MED vs. VDO (JPD)	0.115039	Accept

When computing the PSk and performing the hypotheses tests, we obtain similar results for the Experimental, the Gaussian and the Lorentzian probability distributions and means, however, the JPD model again shows some difference, leading to inconsistencies and the conclusion that the JPD equation may, after all, be a poor fit when compared to the Gaussian and the Lorentzian models, as shown in Table IV.

When looking at the JPD results more closely, we observe that **H0:  $\mu_1 = \mu_2$**  is rejected:

- (a) when comparing the mean PSk values between the experimental ( $\mu_1$ ) and the JPD ( $\mu_2$ ) in the modality MED.
- (b) when comparing the mean PSk values for the modalities of MED ( $\mu_1$ ) and VDO ( $\mu_1$ ).

**Table IV.** It shows the results for the set of tests for equal PSk means and different variance, for 20 participants with  $\alpha = 0.05$ .

TEST	p-value	H0: $\mu_1=\mu_2$
<b>MED vs. VDO (Experimental)</b>	7.35028E-05	Reject
<b>Experimental vs. Gaussian (MED)</b>	0.894525196	Accept
<b>Experimental vs. Gaussian (VDO)</b>	0.7366717	Accept
<b>MED vs. VDO (Gaussian)</b>	8.33E-05	Reject
<b>Experimental vs. Lorentzian (MED)</b>	0.83747489	Accept
<b>Experimental vs. Lorentzian (VDO)</b>	0.672415761	Accept
<b>MED vs. VDO (Lorentzian)</b>	0.000109	Reject
<b>Experimental vs. JPD (MED)</b>	0.000267871	Reject
<b>Experimental vs. JPD (VDO)</b>	0.891639557	Accept
<b>MED vs. VDO (JPD)</b>	0.035899	Reject

## 7. Conclusion & Future Perspectives

We have investigated the possibility that Ji’s Planckian distribution, a generalization of Planck’s law, as shown in [38] (pp. 334-346), could be a good model to characterize the power spectrum of brain dynamics as measured via EEG in the modalities of MED and VDO.

We have chosen this model based on previously successful studies, and particularly because the parameter T (temperature) in Planck’s law, determines the shape of the spectrum or distribution. For us this is crucial, since we conjecture that an equivalent parameter to T, which we refer to as M, a mental parameter (perhaps related to the power of will, commitment or free choice), can be set to different values, which could lead to different kinds of brain dynamics, reflected in different power spectrums, opening the way to scientifically study mind~brain complementarity, meaning, intentional action, and even more, spiritual experience and spiritual meanings and values that lead to refined intentions and actions in the world. We foresee that Peirce’s theory of signs will be crucial in this undertaking [39].

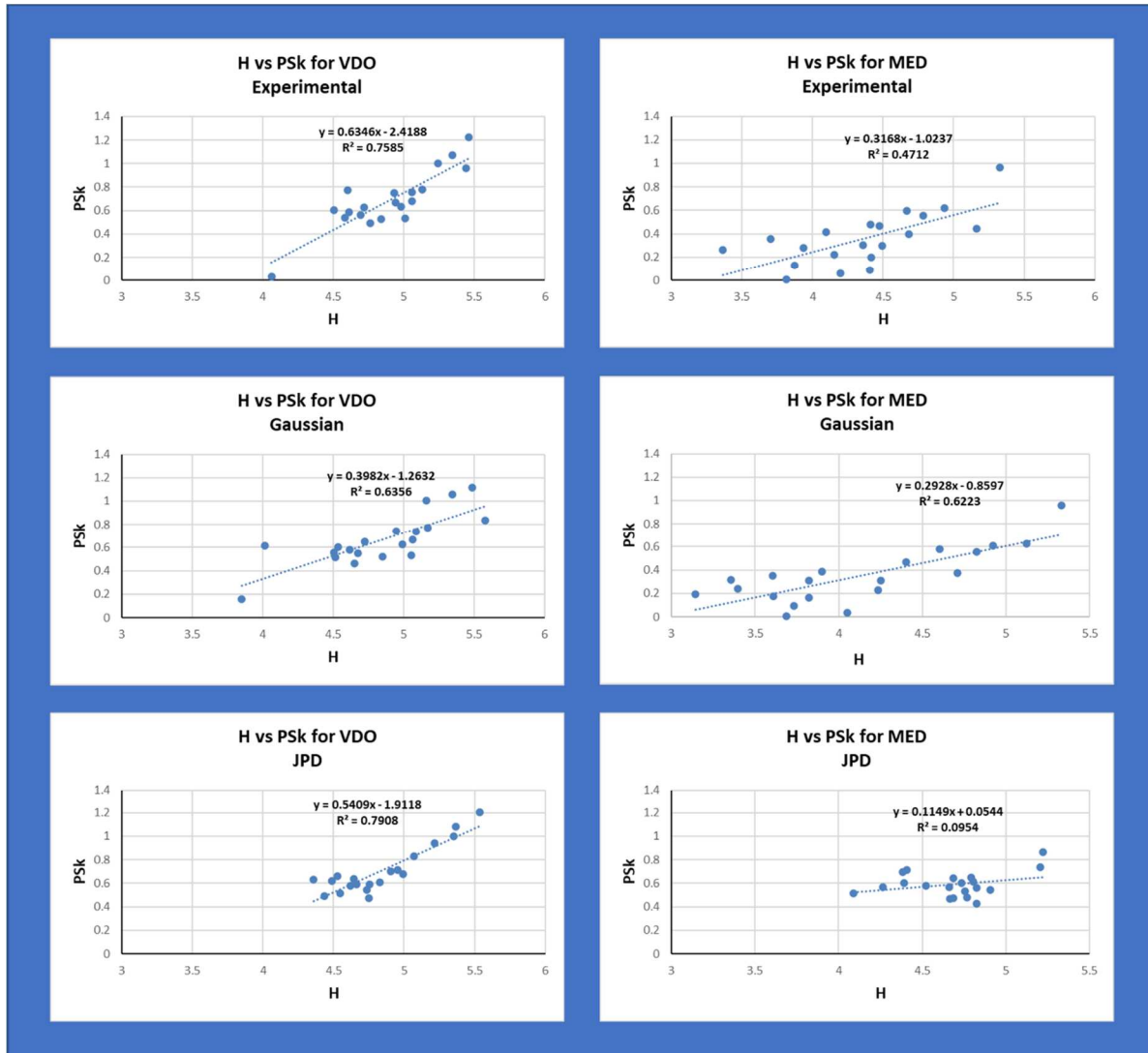


**Figure 7.** It shows H vs. PSk linear fits with equations and R<sup>2</sup>, where the left column shows the Experimental data (top), the Gaussian fit (middle) and the JPD fit (bottom) for the VDO modality, while the right column shows the Experimental data (top), the Gaussian fit (middle) and the JPD fit (bottom) for the MED modality.

We found that the Gaussian and Lorentzian equations were better fits to the experimental data than the JPD, perhaps because EEG brain data is mainly dominated by Gaussian noise, as described by [30] formalized in the study of ‘Statistical Properties of Random Noise Currents’ as treated by Rice [40] and colleagues [41].

It is possible that Ji’s Planckian distribution may be buried in Gaussian noise, something that Ji may have dealt with indirectly in describing his “Planckian Information (IP) index as a new measure of organization” [38] as:

$$I_P = \log_2 \left[ \frac{\int JPD(x)dx}{\int G(x)dx} \right] \tag{19}$$

This is outside of the scope of this work and remains a subject for future studies.

At this stage it is important to mention that the notion of Planckian Information of the Second Kind (IPS), is related to the organized complexity of Weaver [42] whereas Shannon Information (H) is related to disorganized complexity, as explained in [43] and [38] (p. 18).

Based on the above, a bi-dimensional analysis of H vs. IPS may reveal properties in brain dynamics associated with Ji's superstructures [44], where we may be able to differentiate between the modalities MED and VDO qualitatively and quantitatively, as shown in Figure 7, where PSk is a substitute for IPS, since  $IPS = -\log_2(PSk)$ .

Based on Figure 7, we observe in Table V, the values for the  $R^2$  coefficients and slopes for the linear fits (Experimental, Gaussian and JPD) for the VDO and MED modalities. The values of H and PSk for the VDO modality are, in general, larger than for the MED modality. Also very important is the fact that the slope for the linear fits in the VDO modality are significantly greater than the slopes for the MED modality, particularly for the Experimental data and the JPD fit. This is quite interesting since, as we mentioned before in Tables III and IV, the Gaussian fit appeared to be a better fit than the JPD fit, however, in this new analysis we see that the JPD values for  $R^2$  and the slope, are better classifiers for the behavior of the VDO and the MED modalities.

**Table V.** It shows the  $R^2$  coefficients and the slope of the linear fits for the Experimental data, the Gaussian fit and the JPD fit, for the VDO and MED modalities.

	<b><math>R^2</math> for VDO / MED</b>	<b>Slope for VDO / MED</b>
<b>Experimental Data</b>	0.7585 / 0.4712	0.6346 / 0.3168
<b>Gaussian Fit</b>	0.6356 / 0.6223	0.3982 / 0.2928
<b>JPD Fit</b>	0.7908 / 0.0954	0.5409 / 0.1149

This type of analysis is very promising for future EEG studies in multiple modalities, and we conclude that still the JPD may result in an appropriate model for EEG brain dynamics, when studying the mind~brain complementarity, even in the presence of strong Gaussian noise, in order to illustrate or show the influence of mental choices on the dynamics of the brain.

## References

1. Ji, S. (2015). Planckian distributions in molecular machines, living cells, and brains: The wave-particle duality in biomedical sciences. *New Developments in Biology, Biomedical & Chemical Engineering and Materials Science*, (pp. 115-137). Vienna. Retrieved from <https://www.inase.org/library/2015/vienna/bypaper/BICHE/BICHE-17.pdf>
2. Planck, M. (1914). *The Theory of Heat Radiation*. (M. Masius, Trans.) Philadelphia: P. Blakiston's Son & Co.
3. Planck, M. (1915). *Eight Lectures on Theoretical Physics*. (A. P. Wills, Trans.) New York: Columbia University Press.
4. Britannica, The Editors of Encyclopaedia. (2015, May 29). *Double-Aspect Theory*. Retrieved June 30, 2023, from Encyclopedia Britannica: <https://www.britannica.com/topic/double-aspect-theory>

5. Britannica, The Editors of Encyclopaedia. (2020, May 2). *Thomism summary*. Retrieved June 30, 2023, from Encyclopedia Britannica: <https://www.britannica.com/summary/Thomism>
6. Britannica, The Editors of Encyclopaedia. (2014, August 18). *Cartesianism summary*. Retrieved June 30, 2023, from Encyclopedia Britannica: <https://www.britannica.com/summary/Cartesianism>
7. Stang, N. F. (2016, March 4). *Kant's Transcendental Idealism*. Retrieved July 2, 2023, from Stanford Encyclopedia of Philosophy: <https://plato.stanford.edu/entries/kant-transcendental-idealism/>
8. Britannica, The Editors of Encyclopaedia. (2020, February 14). *Transcendental Idealism*. Retrieved June 30, 2023, from Encyclopedia Britannica: <https://www.britannica.com/topic/transcendental-idealism>
9. Stubenberg, L., & Wishon, D. (2023, January 31). *Neutral Monism*. Retrieved July 2, 2023, from Stanford Encyclopedia of Philosophy: <https://plato.stanford.edu/entries/neutral-monism/>
10. Toadvine, T. (2016, September 14). *Maurice Merleau-Ponty*. Retrieved June 30, 2023, from Stanford Encyclopedia of Philosophy: <https://plato.stanford.edu/entries/merleau-ponty/>
11. Kelso, J. A. S., & Engström, D. A. (2006). *The Complementary Nature*. Cambridge, MA: MIT Press.
12. Pribram, K. H. (1954). Toward a Science of Neuropsychology (Method and Data). In R. Patton (Ed.), *Current Trends in Psychology and the Behavioral Sciences* (pp. 115-142). Pittsburgh, PA: University of Pittsburgh Press. Retrieved from <http://www.karlpribram.com/wp-content/uploads/pdf/theory/T-002.pdf>
13. Pribram, K. H. (1971). *Languages of the Brain: Experimental Paradoxes and Principles in Neuropsychology*. Englewood Cliffs, NJ: Prentice-Hall.
14. Pribram, K. H. (1976). Mind, It Does Matter. In S. F. Spicker, & H. T. Englehardt Jr. (Eds.), *Philosophical Dimensions of the Neuro-Medical Sciences. Philosophy and Medicine* (Vol. 2, pp. 97-111). Dordrecht: Springer. [https://doi.org/10.1007/978-94-010-1473-1\\_7](https://doi.org/10.1007/978-94-010-1473-1_7)
15. Pribram, K. H. (1977). Some Observations on the Organization of Studies of Mind, Brain, and Behavior. In N. E. Zinberg (Ed.), *Alternate States of Consciousness* (pp. 220-229). New York: Free Press. Retrieved from <http://karlpribram.com/wp-content/uploads/pdf/theory/T-088.pdf>
16. Pribram, K. H. (2013). *The Form Within: My Point of View*. Westport, CT: Prospecta Press.
17. Pribram, K. H. (1980). Mind, Brain, and Consciousness: The Organization of Competence and Conduct. In J. M. Davidson, & R. J. Davidson (Eds.), *The Psychobiology of Consciousness* (pp. 47-63). Boston, MA: Springer.
18. Eccles, J. C. (1992). Evolution of consciousness. *Proceedings of the National Academy of Sciences of the United States of America*, 89 (16), 7320-7324. <https://doi.org/10.1073/pnas.89.16.7320>
19. Freeman, W. J. (2008). Nonlinear Brain Dynamics and Intention According to Aquinas. *Mind and Matter*, 6 (2), 207-234. Retrieved from <https://www.ingentaconnect.com/content/imp/mm/2008/00000006/00000002/art00005>
20. Merleau-Ponty, M. (1962). *Phenomenology of Perception*. (C. Smith, Trans.) London: Routledge.
21. Freeman, W. J. (2003). A Neurobiological Theory of Meaning in Perception. Part 1: Information and Meaning in Nonconvergent and Nonlocal Brain Dynamics. *International Journal of Bifurcation and Chaos*, 13 (9), 2493-2511. <https://doi.org/10.1142/S0218127403008144>

22. Freeman, W. J., & Vitiello, G. (2016). Matter and Mind are Entangled in Two Streams of Images Guiding Behavior and Informing the Subject Through Awareness. *Mind and Matter*, 14 (1), 7-24. Retrieved from <https://www.ingentaconnect.com/contentone/imp/mmm/2016/00000014/00000001/art00002>
23. Freeman, W. J. (2005). A field-theoretic approach to understanding scale-free neocortical dynamics. *Biological Cybernetics*, 92 (6), 350–359. <https://doi.org/10.1007/s00422-005-0563-1>
24. Freeman, W. J. (1999). Consciousness, intentionality and causality. *Journal of Consciousness Studies*, 6 (11-12), 143-172. Retrieved from <https://www.ingentaconnect.com/contentone/imp/jcs/1999/00000006/f0020011/995>
25. Freeman, W. J. (2009). Deep analysis of perception through dynamic structures that emerge in cortical activity from self-regulated noise. *Cognitive Neurodynamics*, 3 (1), 105–116. <https://doi.org/10.1007/s11571-009-9075-3>
26. Freeman, W. J. (2004). How and Why Brains Create Meaning from Sensory Information. *International Journal of Bifurcation and Chaos*, 14 (2), 515–530. <https://doi.org/10.1142/S0218127404009405>
27. Freeman, W. J. (1975). *Mass Action in the Nervous System: Examination of The Neurophysiological Basis of Adaptive Behavior through the EEG*. New York: Academic Press.
28. Núñez, R. E., & Freeman, W. J. (1999). Restoring to cognition the forgotten primacy of action, intention and emotion. *Journal of Consciousness Studies*, 6 (11-12), ix-xx. Retrieved from <https://www.ingentaconnect.com/contentone/imp/jcs/1999/00000006/F0020011/986>
29. Freeman, W. J., & Vitiello, G. (2016, January). *Matter and Mind are Entangled in EEG Amplitude Modulation and its Double*. Retrieved July 2, 2023, from ResearchGate: [https://www.researchgate.net/publication/290428630\\_Matter\\_and\\_Mind\\_are\\_Entangled\\_in\\_EEG\\_Amplitude\\_Modulation\\_and\\_its\\_Double\\_Preprint\\_Univty\\_California\\_at\\_Berkeley\\_CA\\_USA](https://www.researchgate.net/publication/290428630_Matter_and_Mind_are_Entangled_in_EEG_Amplitude_Modulation_and_its_Double_Preprint_Univty_California_at_Berkeley_CA_USA)
30. Freeman, W. J., & Zhai, J. (2009). Simulated power spectral density (PSD) of background electrocorticogram (ECoG). *Cognitive Neurodynamics*, 3 (1), 97-103. <https://doi.org/10.1007/s11571-008-9064-y>
31. Kozma, R., Freeman, W. J., Davis, J. J., & Lin, C. T. (2014). Model-based measurement of EEG data from linear high-density array (Poster Presentation). *Society for Neuroscience Annual Meeting*. Washington, DC.
32. Kozma, R., Davis, J. J., Lin, C.T., Liao, L.D., & Freeman, W. J. (2013). Optimizing EEG/EMG signal to noise ratio at high spatial resolution. *Society for Neuroscience Congress*, #586.12/NNN11. San Diego.
33. Kozma, R., & Davis, J. J. (2012). On the invariance of cortical synchronization measures across a broad range of frequencies. *4th International Conference on Awareness Science and Technology (iCAST)* (pp. 280-285). Seoul: IEEE. <https://www.doi.org/10.1109/iCAwST.2012.6469627>
34. Davis, J. J., Kozma, R., & Florian, S. (2023). Analysis of Meditation vs. Sensory Engaged Brain States Using Shannon Entropy and Pearson's First Skewness Coefficient Extracted from EEG Data. *Sensors*, 23 (3), 1-23. <https://doi.org/10.3390/s23031293>

35. Davis, J. J. J., Schübeler, F., & Kozma, R. (2019). Psychophysiological Coherence in Community Dynamics – A Comparative Analysis between Meditation and Other Activities. *OBM Integrative and Complementary Medicine*, 4 (1), 1-24. <http://dx.doi.org/10.21926/obm.icm.1901015>
36. Davis, J. J. J., Kozma, R., & Schübeler, F. (2019). Stress Reduction, Relaxation, and Meditative States Using Psychophysiological Measurements Based on Biofeedback Systems via HRV and EEG. In N. Lee (Ed.), *Encyclopedia of Computer Graphics and Games*. Cham: Springer. [https://doi.org/10.1007/978-3-319-08234-9\\_330-1](https://doi.org/10.1007/978-3-319-08234-9_330-1)
37. Davis, J. J., & Kozma, R. (2012). Analysis of phase relationship in ECoG using Hilbert transform and information theoretic measures. *The 2012 International Joint Conference on Neural Networks (IJCNN)* (pp. 1-7). Brisbane: IEEE. <https://doi.org/10.1109/IJCNN.2012.6252486>
38. Ji, S. (2018). *The Cell Language Theory: Connecting Mind and Matter*. London: World Scientific Publishing Europe Ltd.
39. Peirce, C. S. (1931-1958). *The Collected Papers of Charles Sanders Peirce*. (C. Hartshorne, P. Weiss, & A. W. Burks, Eds.) Cambridge, MA: Harvard University Press.
40. Rice, S. O. (1944). Mathematical analysis of random noise. *The Bell System Technical Journal*, 23 (3), 282-332. <https://doi.org/10.1002/j.1538-7305.1944.tb00874.x>
41. Middleton, D. (1988). S.O. Rice and the theory of random noise: Some personal recollections. *IEEE Transactions on Information Theory*, 34 (6), 1367–1373. <https://doi.org/10.1109/18.21273>
42. Weaver, W. (1991). Science and Complexity. In G. J. Klir, *Facets of Systems Science* (pp. 449–456). Boston, MA: Springer.
43. Ji, S. (2018). RASER Model of Single-Molecule Enzyme Catalysis and Its Application to the Ribosome Structure and Function. *Archives of Molecular Medicine and Genetics (AMMG)*, 1 (1), 31-39. Retrieved from <https://hendun.org/admin/uploads/source/AMMG-18-1-104.pdf>
44. Ji, S. (2020). The Planck-Shannon Plot: A Quantitative Method for Identifying ‘Superstructures’ in Cell Biology and Consciousness Study. *Cosmos and History: The Journal of Natural and Social Philosophy*, 16 (2), 142–164. Retrieved from <https://cosmosandhistory.org/index.php/journal/article/view/793>